ZIBELINE INTERNATIONAL™ PUBLISHING

ISSN: 2521-5051 (Print)
ISSN: 2521-506X (Online)
CODEN: ASMCCQ

Acta Scientifica Malaysia (ASM)

DOI: http://doi.org/10.26480/asm.02.2025.100.108

RESEARCH ARTICLE

OPTIMIZATION OF PINEAPPLE LEAF FIBER (ANANAS COMOSUS) IN NATURAL RUBBER COMPOSITES: STRUCTURAL, MORPHOLOGICAL CHARACTERIZATION AND MECHANICAL PROPERTIES

Iyobosa Gift Okunzuwa[a], Aminat Omuwa Abdulwahab[a], Bakoye Yaou[b], Oghenetejiri Oyawiri[a], Oghenetega Ohwo[c], Caleb Eshiayeremia Kayode[a], Samuel Ikponmwosa Okunzuwa[d]

[a] Department of Chemistry, Faculty of Physical Sciences, University of Benin, Benin City, Nigeria.
[b] Department of Chemistry, Faculty of Sciences and Technology, University Dan Dicko Dankouloudo of Maradi, Maradi (Niger)
[c] Department of Chemical Sciences, Faculty of Basic and Applied sciences, University of Africa, Toru-Orua, Sagbama. Nigeria.
[d] Department of Physics, Faculty of Physical sciences, University of Benin, Benin City, Nigeria.
**Corresponding Author email: iyobosa.iyawe@uniben.edu*

ARTICLE DETAILS

Article History:

Received 10 June 2025
Revised 15 July 2025
Accepted 29 August 2025
Available online 27 September 2025

ABSTRACT

Natural rubber composites reinforced with pineapple leaf fibre (PALF) were investigated using Fourier Transform Infrared Spectroscopy (FTIR), Scanning Electron Microscopy (SEM), and Energy-Dispersive Spectroscopy (EDS). Mechanical properties, including tensile strength, elongation at break, impact resistance, hardness, flexural strength, and elastic modulus, were evaluated for composites containing 0–4 g PALF. FTIR revealed a shift in O–H stretching from 3350.9 cm^{-1} (0 g) to 3306.1 cm^{-1} (4 g), indicating enhanced hydrogen bonding and fibre–matrix adhesion. The disappearance of the C≡C/C≡N band in reinforced samples confirmed chemical stabilisation and fibre incorporation. SEM showed smooth morphology in unreinforced rubber, while PALF composites exhibited rougher surfaces with embedded fibres, alongside regions of fibre pull-out and agglomeration. EDS confirmed increased carbon and oxygen content in reinforced samples, consistent with cellulose incorporation.

Tensile strength and elongation at break increased to maxima at 2 g PALF (11.80 MPa, 386%) before declining at higher loadings due to agglomeration. In contrast, impact resistance, hardness, flexural strength, and elastic modulus increased monotonically, with impact resistance reaching 0.90 MPa at 4 g. Moderate PALF loading (≤2 g) provides optimal strength–flexibility balance, while higher contents enhance rigidity at the expense of elasticity, demonstrating PALF's potential as a sustainable rubber reinforcement.

KEYWORDS

Natural rubber composite; pineapple leaf fibre (PALF); characterization; mechanical properties; sustainable reinforcement.

1. INTRODUCTION

The increasing global demand for sustainable and environmentally friendly materials has led to extensive research into the development of green composites. One promising area of focus is the reinforcement of natural rubber with plant-based fibers, which not only enhances composite performance but also promotes environmental sustainability as demonstrated by most of researcher (Mohanty et al., 2002; John and Thomas 2008). The urgency for alternative materials arises from growing concerns about synthetic fibers, particularly their non-biodegradability and reliance on petrochemical resources as demonstrated by (Bledzki and Gassan 1999).

Natural rubber, derived from *Hevea brasiliensis*, is widely used in industrial applications due to its elasticity, resilience, and durability. However, in its pure form, natural rubber has limitations such as low modulus and vulnerability to environmental degradation. Traditionally, synthetic fillers like carbon black and silica have been used to improve rubber's performance. Despite their effectiveness, these reinforcements contribute to environmental degradation due to their non-biodegradability and energy-intensive production processes as demonstrated by (Bhowmick and Stephens, 2001). In contrast, natural fibers provide a sustainable alternative as they are biodegradable, renewable, and have a lower environmental footprint as demonstrated (Abdul Khalil et al., 2012)

Among various natural fibers, pineapple leaf fiber (PALF), derived from *Ananas comosus* (L.) Merr. [Synonym: Ananas sativus (Schult. & Schultz. f.) Lindl. ex-Beer], has emerged as a promising reinforcement material. Belonging to the family Bromeliaceae, pineapple is widely cultivated in tropical regions, and its agricultural byproduct—the leaves—serves as an abundant source of fibrous material. PALF is particularly attractive due to its high cellulose content, tensile strength, and availability in countries like Nigeria, making it an eco-friendly and cost-effective solution for composite development as demonstrated (Reddy and Yang, 2005).

Rubber composites are widely used in industries such as automotive, construction, and packaging due to their excellent elasticity, durability, and resistance to environmental degradation. In the automotive sector, rubber composites are utilized in tires, seals, vibration dampers, and hoses, enhancing vehicle performance and fuel efficiency as demonstrated by (Visakh and Thomas, 2013). However, the use of synthetic reinforcements in these materials has raised sustainability concerns, leading to increased interest in natural fiber alternatives. Incorporating

Quick Response Code	Access this article online	
	Website: www.actascientificamalaysia.com	**DOI:** 10.26480/asm.02.2025.100.108

Cite The Article: Iyobosa Gift Okunzuwa, Aminat Omuwa Abdulwahab, Bakoye Yaou, Oghenetejiri Oyawiri, Oghenetega Ohwo, Caleb Eshiayeremia Kayode, Samuel Ikponmwosa Okunzuwa (2025). Optimization Of Pineapple Leaf Fiber (Ananas Comosus) In Natural Rubber Composites: Structural, Morphological Characterizatio n And Mechanical Properties. *Acta Scientifica Malaysia, 9(2): 100-108 .*

PALF into rubber matrices presents an opportunity to develop eco-friendly composites, reducing dependence on petrochemical-derived fillers while utilizing agricultural waste efficiently as demonstrated by (George et al., 2001).

Despite its advantages, PALF reinforcement presents challenges, such as poor fiber-matrix adhesion, fiber coagulation, and uneven dispersion, which can impact composite performance as demonstrated by (John and Thomas, 2008). Various fiber modification techniques, including alkali treatment, surface functionalization, and size reduction, have been explored to enhance interfacial bonding and improve fiber dispersion within the rubber matrix as demonstrated by (Joseph et al., 2002; Mishra et al., 2004).

This study focuses on the characterization of PALF-reinforced natural rubber composites, evaluating their structural and thermal properties using Fourier-transform infrared spectroscopy (FTIR), scanning electron microscopy (SEM), and energy-dispersive spectroscopy (EDS). These techniques will provide insights into fiber-matrix interactions, composite morphology, and elemental composition, helping to optimize PALF's application in sustainable composite development (Abdul Khalil et al., 2012; Reddy and Yang, 2005).

2. Materials And Methods

2.1 Sample Collection/Sample Area

The natural rubber latex was sourced from the Rubber Research Institute of Nigeria (RRIN), Benin City, Edo state Nigeria between Latitude 6o08' 11' N Longitude 5o34' 38' E with a dry rubber content of 60%. Pineapple leaf fiber (PALF) was collected from a local fruit seller at Evbuotubu quarters, Benin City, Nigeria and was subjected to processing before use. Additional compounding materials such as zinc oxide (WARCHEM-99% purity), stearic acid (WARCHEM-99% purity), Sulphur (WARCHEM-99% purity), and glycerol (WARCHEM- 98.5% purity) incorporated as additives to enhance the composite properties were sourced from Pyrex-IG Scientific company Benin City, Edo State Nigeria.

Table 1: Compounding Ingredients Adapted From (Barlow 1993)

Ingredients	Parts Hundred Rubber (PHR)	Functional Class
Natural Rubber Latex (conc. 60% dry rubber)	100	Elastomer
Zinc Oxide	5.0	Activator
Stearic acid	2.0	Activator
Sulphur	2.5	Vulcanizing agent
PALF	(0.00, 0.86, 1.72, 2.58, 3.44)	Reinforcer
Glycerol	5.42	Plasticizer

2.2 Preparation of Pineapple Leaf Fiber

The extracted PALF was cleaned using a wetting-retting process followed (Ayekpam and Vasugi, 2020) by washing and drying under direct sunlight for 2 hours. The dried fibers were manually chopped into short fibers of approximately 5 mm length to enhance uniform dispersion within the rubber matrix.

2.3 Composite Preparation for Characterization

Natural rubber latex was mixed with compounding additives using a mechanical stirrer. Two weight fractions (0g and 4g) of PALF were gradually added and stirred continuously to ensure uniform dispersion as demonstrated by (Sanusi et al., 2023). The compounded rubber was poured into molds of 0.9cm thick and cured at 90°C for 90 minutes as demonstrated by (Sanusi et al., 2023). The prepared rubber composites were then cooled and conditioned before mechanical and structural characterization.

2.4 Composite Preparation for Mechanical Tests

Natural rubber latex was mixed with compounding additives using a mechanical stirrer. PALF was added at different weight fractions (0g, 1g, 2g, 3g, and 4g), and the mixture was stirred continuously for uniform dispersion. The compounded rubber was poured into molds and cured at 90°C for 90 minutes as demonstrated (Sanusi et al., 2023). The prepared rubber composites were then cooled and conditioned before mechanical characterization.

2.5 Characterization

2.5.1 Fourier-Transform Infrared Spectroscopy

The Fourier-transform infrared spectroscopy (FTIR) analysis was conducted using the Cary 630 FTIR spectrometer (Agilent Technologies, USA). The spectra were recorded in the range of 400–4000 cm^{-1} using the KBr pellet method. This technique was employed to evaluate the functional groups present and to detect any chemical interactions between the natural rubber matrix and pineapple leaf fiber (PALF).

2.5.2 Scanning Electron Microscope (Sem) / Energy-Dispersive X-Ray Spectroscopy (Edx)

The morphological analysis of the rubber composites was conducted using PhenonWorld Eindhoven the Netherlands model phenom ProX. The samples were coated with a thin layer of gold using a sputter coater to improve conductivity before imaging.

2.6 Mechanical Properties

The mechanical properties of the PALF-reinforced natural rubber composites were evaluated to determine the effect of fiber loading on tensile strength, elongation at break, impact resistance, hardness, flexural strength, and elastic modulus. The following tests were conducted using specific instruments to ensure accuracy and reproducibility.

2.6.1 Tensile Strength And Elongation At Break

The tensile test was conducted using a Tensile Strength Test Machine (TM 2101-T7) in accordance with (ASTM). The test was performed with a maximum force of 10 kN. Rectangular test specimens with dimensions 100 mm × 15 mm × 5 mm (length × width × thickness) were prepared. A crosshead speed of 2 mm/min was maintained throughout the test. Each specimen was securely clamped in the grips of the testing machine to prevent slippage. As the test commenced, the machine applied a unidirectional tensile force until specimen failure. The resistance to stretching and elongation was continuously recorded using a load cell.

The following tensile parameters were measured:

- Tensile strength (breaking point)
- Elongation at break (%)
- Tensile modulus (stiffness response)

2.6.2 Impact Resistance

The impact resistance of the composites was evaluated using a Charpy Impact Testing Machine (Cat. Nr. 412) with a 15J capacity, following the standard by (ASTM). Notched test specimens were placed horizontally on the machine's support anvils, ensuring proper alignment. A pendulum hammer was released from a fixed height, striking the specimen at its center. The energy absorbed during fracture was recorded in joules (J), providing a measure of the material's resistance to sudden impact forces.

2.6.3 Hardness

The hardness of the composites was measured using a Durometer (Muver, Model 5019, Serial No. 01554), following the standard by (ASTM). Test

samples were placed on a flat surface, and the durometer indenter was pressed perpendicularly against the sample. The hardness value was recorded after 15 seconds of stabilization to ensure accuracy.

2.6.4 Flexural Strength

The flexural strength of the composites was measured using a Three-Point Bending Test Machine following the standard by (ASTM). Test samples were placed on two support points, and a central force was applied at a constant speed until failure. The maximum stress the material could withstand before breaking was recorded in megapascals (MPa), indicating its ability to resist bending forces.

3. Results And Discussion

The results from the FTIR spectra showed changes in peaks between the 0g and 4g composites, indicating improved fiber matrix interaction.

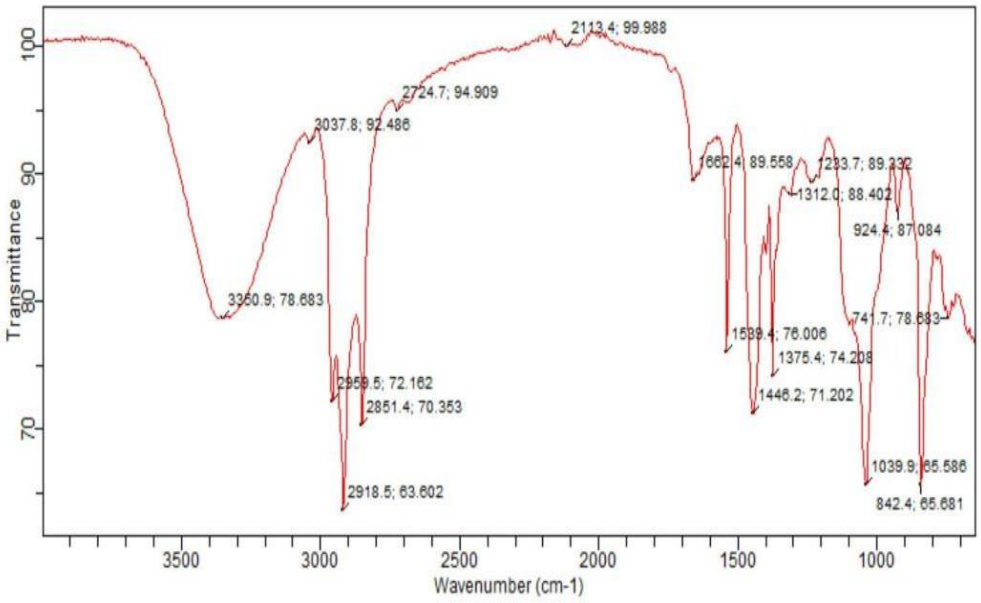

Figure 1: FTIR Spectra of the unreinforced rubber composite (0g PALF)

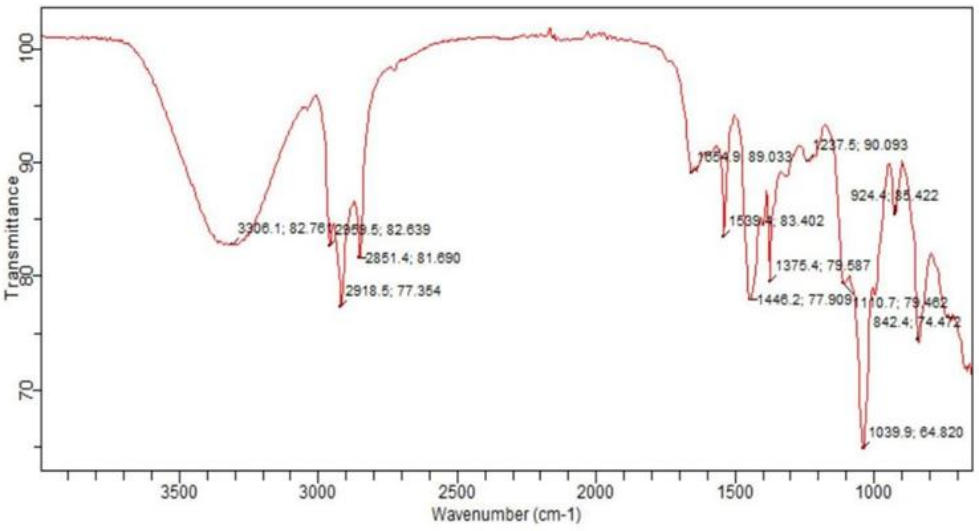

Figure 2: FTIR Spectra of the fiber-reinforced rubber composite (4g PALF)

From Figure 1 and Figure 2, a broad absorption peak was observed at 3350.9 cm^{-1} in the 0g sample, which corresponds to hydroxyl (-OH) and amino (-NH) stretching vibrations from natural rubber and residual moisture. In the 4g sample, this peak shifted to 3306.1 cm^{-1}, suggesting enhanced hydrogen bonding between PALF and the rubber matrix. This shift indicates that the hydroxyl groups in PALF interacted with the functional groups in the rubber, leading to improved fiber-matrix adhesion. The 0g sample exhibited a C=O absorption peak at 1743 cm^{-1}, attributed to the carbonyl functional groups in the natural rubber structure.

In the 4g sample, a new peak emerged at 1644.47 cm^{-1}, corresponding to C=N imine stretching, which was not present in the unreinforced sample. This suggests possible interactions between PALF components and the rubber matrix, potentially forming secondary chemical bonds. In the 4g sample, a peak at 1552.69 cm^{-1} was attributed to the C=C cyclic alkene stretching from PALF components, whereas the C-O ether stretching peak appeared at 1150.38 cm^{-1}. These shifts indicate that PALF's lignocellulosic structure influenced the composite's chemical environment, further supporting fiber-matrix interaction. The 0g sample exhibited a peak at 1022.02 cm^{-1}, attributed to the C-O stretching vibration of primary alcohols. This peak was reduced in intensity in the 4g sample, suggesting a reduction in free hydroxyl groups due to interactions with the rubber matrix.

The results confirm that PALF reinforcement modified the chemical environment of the rubber composite. The shift in hydroxyl (-OH) stretching indicates enhanced hydrogen bonding, while the appearance of the imine (C=N) peak suggests potential secondary bonding interactions. These findings support the successful integration of PALF into the rubber matrix, leading to structural changes that may influence mechanical performance and composite durability.

3.1 Sem Morphological Analysis

The SEM images depicting the surface morphology of the unreinforced rubber composite (0g PALF) and the reinforced rubber composite (4g PALF)

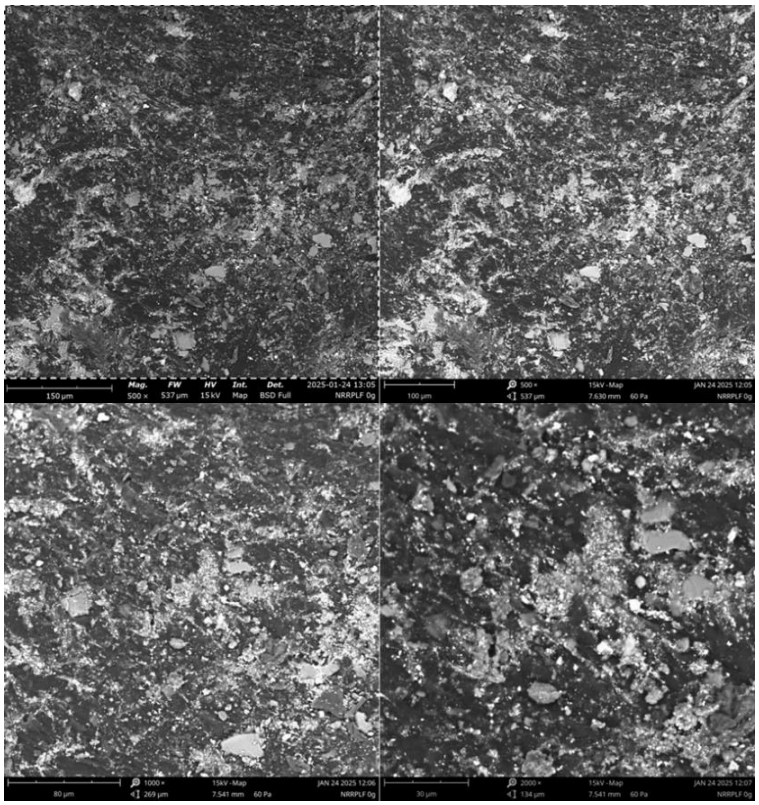

Figure 3: Morphology of unreinforced rubber composite (0g PALF) at 150, 100, 80 and 30 m.

From Figure 3, the unreinforced rubber composite exhibited a smooth and compact surface, indicating the absence of fiber reinforcement. The rubber matrix appeared uniform, with minimal surface roughness and no visible fiber structures. Some micropores were observed, suggesting limited internal support, which may contribute to lower mechanical strength.

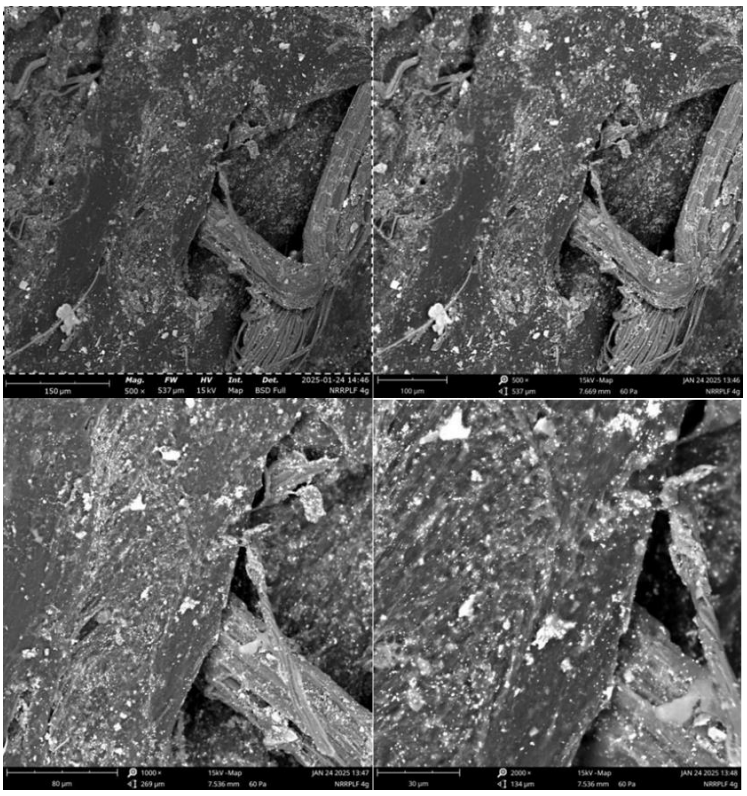

Figure 4: Morphology of fiber-reinforced rubber composite (4g PALF) at 150, 100, 80 and 30 m.

From Figure 4, the reinforced rubber composite displayed a rougher surface texture, with well- embedded PALF fibers visible within the rubber matrix. The presence of fiber pull-out in some regions indicated areas of weak fiber-matrix bonding, likely due to uneven dispersion or insufficient interfacial adhesion. However, reduced porosity compared to the 0g sample suggested improved structural integrity. Some fiber agglomeration was noted, which could create stress concentration points, potentially affecting composite performance.

3.2 Eds Elemental Composition Analysis

Energy-dispersive X-ray spectroscopy (EDS) analysis revealed the elemental composition of both unreinforced (0g PALF) and fiber-reinforced (4g PALF) rubber composite samples, thereby confirming the successful incorporation of PALF incorporation into the rubber matrix.

Table 2: Elemental composition of unreinforced rubber composite (0g PALF)

Element Number	Element Symbol	Atomic Conc.	Weight Conc.
06	C	63.37	41.99
11	Na	8.80	11.16
26	Fe	3.25	10.01
14	Si	6.32	9.79
16	S	4.57	8.08
13	Al	4.65	6.92
12	Mg	3.00	4.03
20	Ca	1.44	3.18
07	N	3.76	2.91
19	K	0.56	1.21
22	Ti	0.27	0.72
25	Mn	0.00	0.00
15	P	0.00	0.00
17	Cl	0.00	0.00

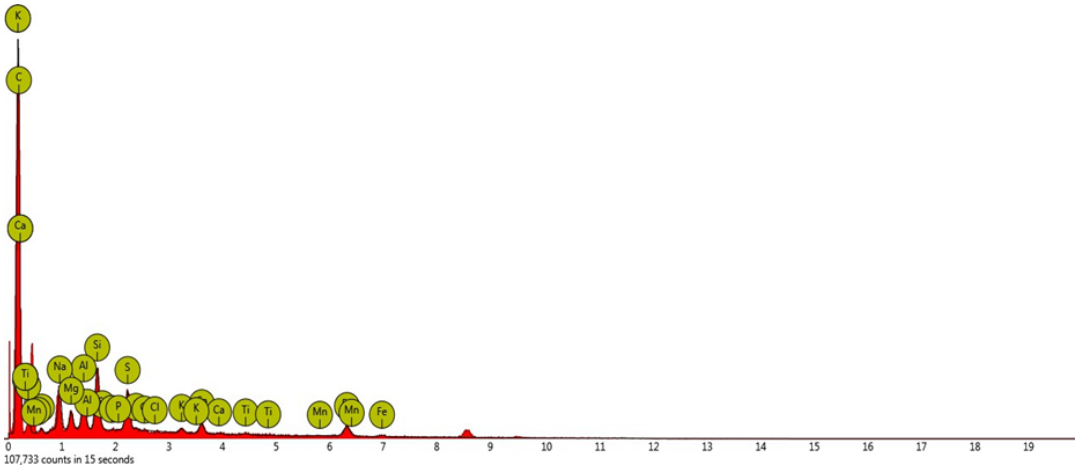

Figure 5: EDS spectra of unreinforced rubber composite (0g PALF)

From Table 2 and Figure 5, high carbon content, primarily from the rubber matrix. Minimal oxygen, silicon, and aluminum levels, consistent with pure rubber composition.

Table 3: Elemental composition of fiber-reinforced rubber composite (4g PALF)

Element Number	Element Symbol	Atomic Conc.	Weight Conc.
06	C	75.99	60.63
11	Na	7.36	11.24
16	S	3.77	8.04
07	N	5.83	5.43
14	Si	2.17	4.05
19	K	1.16	3.01
12	Mg	1.24	2.00
13	Al	1.02	1.83
17	Cl	0.66	1.55
20	Ca	0.49	1.31
26	Fe	0.17	0.61
15	P	0.14	0.29
22	Ti	0.00	0.00
25	Mn	0.00	0.00

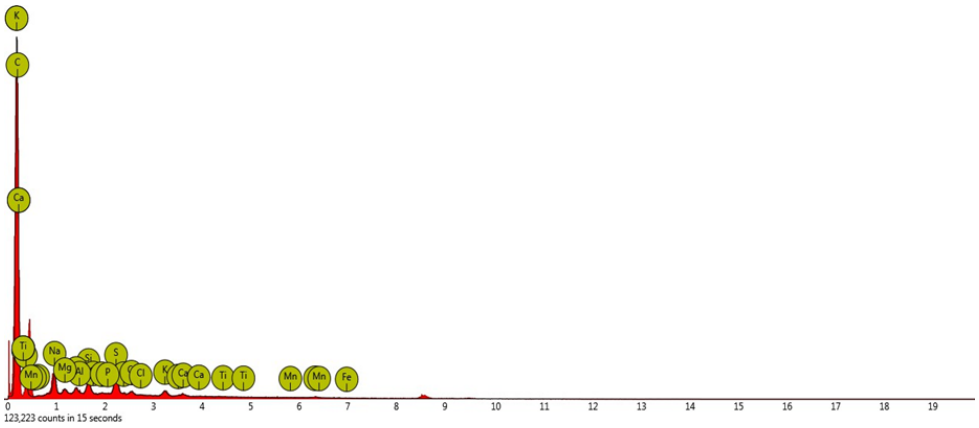

Figure 6: EDS Spectra of fiber-reinforced rubber composite (4g PALF).

From Table 3 and Figure 6 in the 4g sample there is an increased carbon content, confirming PALF reinforcement. Higher oxygen concentration, suggesting the presence of PALF's cellulose, hemicellulose, and lignin components. Reduction in silicon and aluminum levels, indicating compositional changes due to fiber incorporation. SEM images confirm that PALF reinforcement modifies the composite's surface morphology, with better structural integrity but localized fiber agglomeration at higher fiber loading. The EDS results validate fiber incorporation, with increased carbon and oxygen levels reflecting the natural fiber content. These findings support the effectiveness of PALF as a reinforcing agent, though optimization of fiber dispersion is necessary to minimize defects and enhance mechanical performance.

3.3 Tensile Strength and Elongation at Break

Tensile strength increased with fiber content, peaking at 11.80 MPa at 2g PALF loading before declining due to fiber agglomeration at 3g and 4g. These findings align with other studies on natural fiber-reinforced rubber composites, where an optimal fiber loading exists before mechanical performance begins to decline as recently shown by (Mustafa et al., 2020).

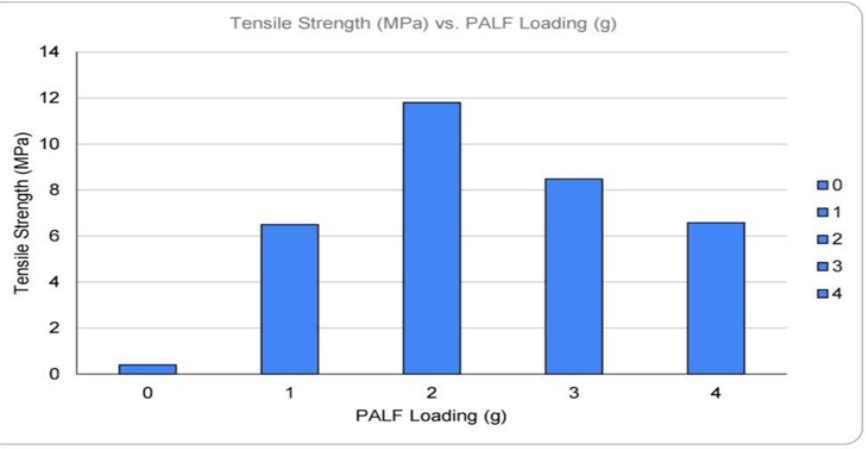

Figure 7: Effect of different loading of PALF on tensile strength

Elongation at break also showed a similar trend with tensile strength. Elongation increased from 334.57% (0g) to 386.17% (2g), indicating improved flexibility due to better stress transfer. However, it dropped at 3g (260.93%) and 4g (224.99%) as fiber agglomeration created stress points and restricted rubber chain mobility. This trend aligns with a study where elongation improves with filler loading up to a limit before declining due to fiber-matrix interaction issues (Mohanty et al., 2002). Moderate PALF reinforcement (≤2g) enhances flexibility, while excessive loading (≥3g) reduces elasticity due to agglomeration.

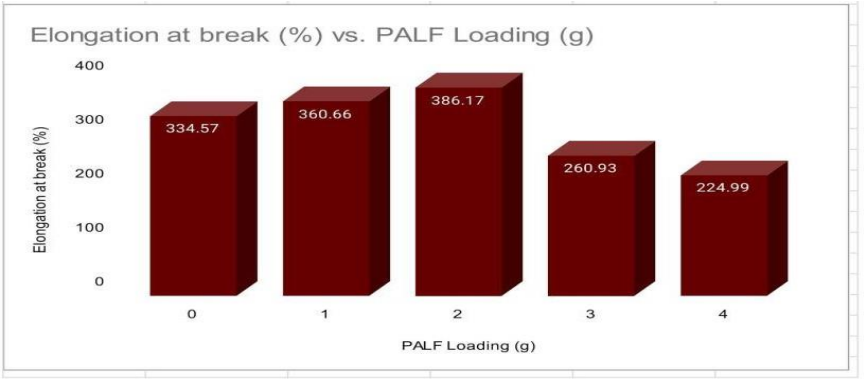

Figure 8: Effect of different loading of PALF on elongation at break.

3.4 Impact Strength

The result of the Impact strength revealed an increased with fiber content, reaching 0.65 MPa at 2g due to well-dispersed fibers improving energy absorption. Strength further rose to 0.90 MPa at 4g, as higher fiber content created a more rigid structure. While fiber agglomeration typically weakens tensile strength, it contributed to localized rigid zones that enhanced impact absorption. However, excessive agglomeration could eventually lead to brittle behavior.

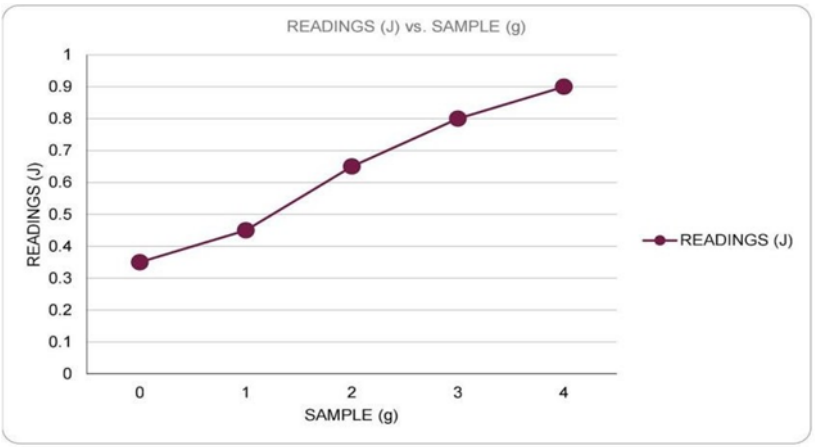

Figure 9: Graph on the effects of different loading of PALF on Impact test.

3.5 Hardness

Hardness increased with PALF content as fibers restricted rubber chain movement, enhancing stiffness. According to a study, higher filler loading reduces elasticity due to restricted molecular mobility and increased cross-linking (Ismail et al., 2005). At 1g and 2g, well-dispersed fibers contributed to hardness, while at 3g and 4g, further rigidity developed despite fiber agglomeration. Unlike tensile strength, which peaked at 2g, hardness continued rising, indicating that while excess fiber weakens bonding, it enhances stiffness. This improves wear resistance but may reduce flexibility, impacting elongation at break and impact strength.

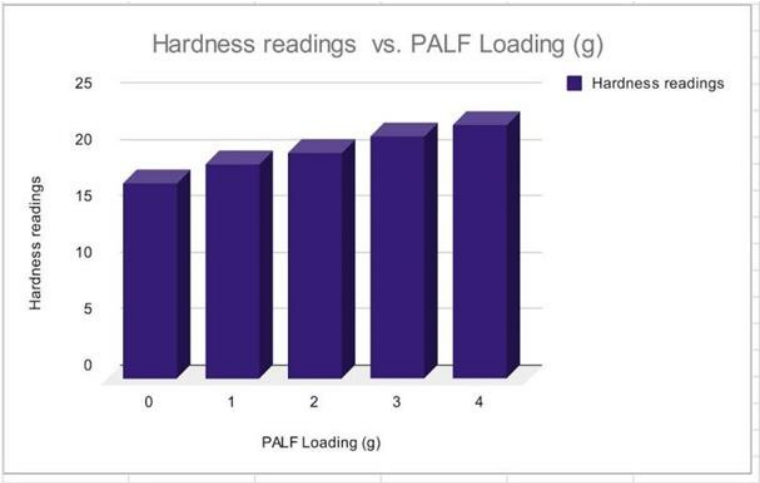

Figure 10: Effects of different loading of PALF on hardness.

3.6 Flexural Strength

Flexural strength increased with PALF content, peaking at 0.026 MPa (4g), with the most significant improvement at 3g and 4g. This suggests that PALF enhances bending resistance by acting as a stiffening agent, improving load distribution, and strengthening fiber-matrix interaction. Lower values at 1g and 2g indicate insufficient reinforcement. However, excessive fiber content may cause agglomeration, leading to uneven stress distribution and reduced flexibility, increasing the risk of cracking under strain.

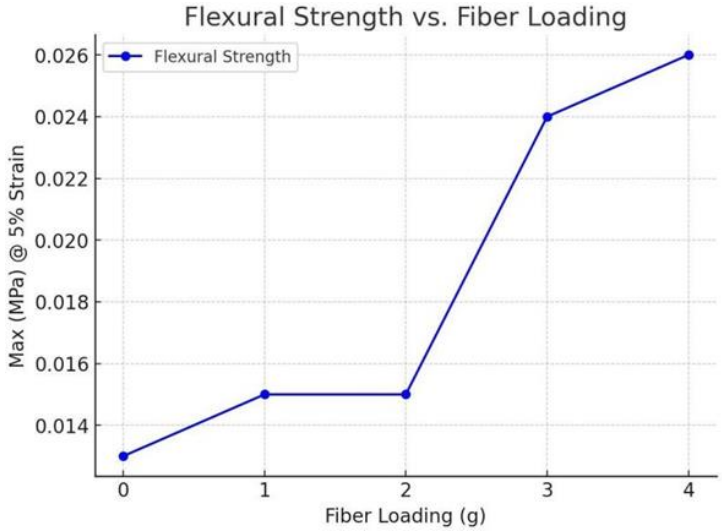

Figure 11: Effects of different loading of PALF on flexural strength

4. Conclusion

This study confirms that pineapple leaf fibre (PALF) reinforcement significantly influences the mechanical properties of natural rubber composites. Moderate fibre loading (≤2 g) optimizes tensile strength, flexibility and impact resistance, while higher contents (≥3 g) enhance hardness and stiffness but reduces elongation at break due to fibre agglomeration and restricted chain mobility. These results highlight PALF's potential as sustainable reinforcement, offering mechanical improvements while serving as a sustainable alternative to synthetic fillers. However, challenges of fibre dispersion and interfacial adhesion remain critical and require further optimization. Future work should focus on fibre surface modification and hybrid reinforcement approaches to overcome these limitations and advance the industrial applications of PALF-reinforced rubber composites.

Acknowledgement

The authors gratefully acknowledge University of Benin, Department of Chemistry for their support on this project.

References

Abdul, K.H.P.S., Bhat, A.H., and Ireana, Y.A.F., 2012. Green composites from sustainable cellulose nanofibrils: A review Carbohydrate Polymers, 87 (2), Pp. 963–979.

ASTM International. Annual book of ASTM standards: Section 8 – Plastics and rubber. ASTM International. Retrieved from www.astm.org

Barlow, F.W., 1993. Rubber Compounding: Principles, Materials, and Techniques (2nd ed.). CRC Press Taylor and Francis Group.

Bhowmick, A.K., and Stephens, H.L., 2001. Handbook of Elastomers. CRC Press.

Bledzki, A.K., and Gassan, J., 1999. Composites reinforced with cellulose-based fiber. Progress in Polymer Science, 24 (2), Pp. 221–274.

George, J., Sreekala, M.S., and Thomas, S., 2001. A review on interface modification and characterization of natural fiber-reinforced plastic composites. Polymer Engineering and Science, 41 (9), Pp. 1471–1485.

Ismail, H., Osman, H., and Ariffin, A., 2005. A comparative study on curing characteristics, mechanical properties, swelling behavior, thermal stability, and morphology of feldspar and silica in SMR L vulcanizates. Journal of Applied Polymer Science, 43 (5), Pp. 1323–1344.

John, M.J., and Thomas, S., 2008. Biofibres and biocomposites. Carbohydrate Polymers, 71 (3), Pp. 343–364.

Joseph, P.V., Rabello, M.S., Mattoso, L.H.C., Joseph, K., and Thomas, S., 2002. Environmental effects on the degradation behavior of sisal fiber reinforced with polypropylene composite. Composites Science and Technology, 62 (10), Pp. 1357–1372.

Joyshree A., and Vasugi, N., 2020. Extraction of Neem Twigs Fiber. SSRG International Journal of Polymer and Textile Engineering (SSRG-IJPTE) – Volume 7 Issue 1 – Jan - April 2020

Mishra, S., Tripathy, S.S., Nayak, S.K., and Satapathy, A.K., 2004. Novel eco-friendly bio composites: Biofiber reinforced biodegradable polyester amide composites—fabrication and properties evaluation. Journal of Reinforced Plastics and Composites, 23 (15), Pp. 1601–1610.

Mohanty, A.K., Misra, M., and Drzal, L.T., 2002. Sustainable bio-composites from renewable resources: Opportunities and challenges in the green materials world. Journal of Polymers and the Environment, 10 (1-2), Pp. 19–26.

Muniandy, K., Ismail, H., and Othman, N., 2012. Effects of partial replacement of rattan powder by commercial fillers on the properties of natural rubber composites. Bioresources, 7 (4), Pp. 4640– 4657.

Mustafa, M.S., Ismail, S.N.S., Shaipul A.S.M., Abdul Wahab, N.M., Majid, N.A., and Sarip, M.N., 2020. Pineapple leaf fibre filled natural rubber composite: The effect of filler loading. In Charting the Sustainable Future of ASEAN in Science and Technology (pp. 447– 454). Springer.

Reddy, N., and Yang, Y., 2005. Biofibers from agricultural byproducts for industrial applications. Trends in Biotechnology, 23 (1), Pp. 22–27.

Syafiqah, N.M.S., Mohamad, N.M.Y., and Zainathul, A.S.A.S., 2023. Potential Bio-filler Cellulose Derived from Cucumber Pomace Filled Natural Rubber Latex Films. Malaysian Journal of Chemistry, 25 (3), Pp. 87-96.

Visakh, P.M., Thomas, S., Aji, P.M., Arup, K.C., 2013. Advances in elastomers I: Blends and interpenetrating networks. Springer.